

UCLA

Papers

Title

Dynamic Fine-Grained Localization in Ad-Hoc Wireless Sensor Networks

Permalink

<https://escholarship.org/uc/item/6xs0j41x>

Authors

Savvides, Andreas
Han, Chih-Chieh
Srivastava, Mani B.

Publication Date

2001-05-05

Peer reviewed



Dynamic Fine-Grained Localization in Ad-Hoc Networks of Sensors

Andreas Savvides, Chih-Chieh Han and Mani B. Strivastava
Networked and Embedded Systems Lab
Department of Electrical Engineering
University of California, Los Angeles
{asa,vvide, simonhan, mbs}@ee.ucla.edu

ABSTRACT

The recent advances in radio and embedded system technologies have enabled the proliferation of wireless sensor networks. Such wirelessly connected sensors are released in many diverse environments to perform various monitoring tasks. In many such tasks, location awareness is inherently one of the most essential system parameters. It is not only needed to report the origins of events, but also to assist group querying of sensors, routing, and to answer questions on the network coverage. In this paper we present a novel approach to the localization of sensors in an ad-hoc network. We describe a system called AHLoS (Ad-Hoc Localization System) that enables sensor nodes to discover their locations using a set of distributed iterative algorithms. The operation of AHLoS is demonstrated with an accuracy of a few centimeters using our prototype testbed while scalability and performance are studied through simulation.

Keywords

location discovery, localization, wireless sensor networks

1. INTRODUCTION

1.1 Sensor Networks and Location Discovery

No wadays, wireless devices enjoy widespread use in numerous diverse applications including that of sensor networks. The exciting new field of *wireless sensor networks* breaks away from the traditional end-to-end communication of voice and data systems, and introduces a new form of distributed information exchange. Myriads of tiny embedded devices, equipped with sensing capabilities, are deployed in the environment and organize themselves in an ad-hoc network. Information exchange among collaborating sensors becomes the dominant form of communication, and the network essentially behaves as a large, distributed computation machine. Applications featuring such networked devices are becoming increasingly prevalent, ranging from environmental and natural habitat monitoring, to home networking,

medical applications and smart battlefields. Networked sensors can signal a machine malfunction to the control center in a factory, or alternatively warn about smoke on a remote forest hill indicating that a dangerous fire is about to start. Other wireless sensor nodes can be designed to detect the ground vibrations generated by the silent footsteps of a cat burglar and trigger an alarm.

Naturally, the question that immediately follows the actual detection of events, is: *where?* Where are the abnormal vibrations detected, where is the fire, which house is about to be robbed? To answer this question, a sensor node needs to possess knowledge of its physical location in space. Furthermore, in large scale ad-hoc networks, knowledge of node location can assist in routing [5] [6], it can be used to query nodes over a specific geographical area or it can be used to study the coverage properties of a sensor network [31]. Additionally, we envision that location awareness developed here will enjoy a wide spectrum of applications. In tactical environments, it can be used to track the movements of targets. In a smart kindergarten [32] it can be used to monitor the progress of children by tracking their interaction with toys and with each other; in hospitals it can keep track of equipment, patients, doctors and nurses or it can drive context aware services similar to the ones described in [4], [29].

The incorporation of location awareness in wireless sensor networks is far from a trivial task. Since the network can consist of a large number of nodes that are deployed in an ad-hoc fashion, the exact node locations are not known a-priori. Unfortunately, the straightforward solution of adding GPS to all the nodes in the network is not practical since:

- GPS cannot work indoors or in the presence of dense vegetation, foliage or other obstacles that block the line-of-sight from the GPS satellites.
- The power consumption of GPS will reduce the battery life on the sensor nodes thus reducing the effective lifetime of the entire network.
- The production cost factor of GPS can become an issue when large numbers of nodes are to be produced.
- The size of GPS and its antenna increases the sensor node form factor. Sensor nodes are required to be small and inobtrusive.

Permission to make digital or hard copies of part or all of this work or personal or classroom use is granted without fee provided that copies are not made or distributed for profit or commercial advantage and that copies bear this notice and the full citation on the first page. To copy otherwise, to republish, to post on servers, or to redistribute to lists, requires prior specific permission and/or a fee.

ACM SIGMOBILE 7/01 Rome, Italy

© 2001 ACM ISBN 1-58113-422-3/01/07...\$5.00

To this end, we seek an alternative solution to GPS that is low cost, rapidly deployable and can operate in many diverse environments without requiring extensive infrastructure support.



Figure 1: WINS Sensor Node from RSC

1.2 Our Work

We propose a new distributed technique that only requires a limited fraction of the nodes (beacons) to know their exact location (either through GPS or manual configuration) during deployment and that nevertheless can attain network-wide fine-grain location awareness. Our technique, which we call AHLoS (Ad-Hoc Localization System), relieves the drawbacks of GPS as it is low cost, it can operate indoors and does not require expensive infrastructure or pre-planning. AHLoS enables nodes to dynamically discover their own location through a two-phase process, ranging and estimation. During the ranging phase, each node estimates its distance from its neighbors. In the estimation phase, nodes with unknown locations use the ranging information and known beacon node locations in their neighborhood to estimate their positions. Once a node estimates its position it becomes a beacon and can assist other nodes in estimating their positions by propagating its own location estimate through the network. This process iterates to estimate the locations of as many nodes as possible.

The first part of our work examines the ranging challenges. Since almost all ranging techniques rely on signal propagation characteristics, they are susceptible to external biases such as interference, shadowing and multipath effects, as well as environmental variations such as changes in temperature and humidity. These physical effects are difficult to predict and depend greatly on the actual environment in which the system is operated. It is therefore critical to characterize the behavior of different ranging alternatives experimentally in order to determine their usefulness in sensor networks. To justify our ranging choice we performed a detailed comparison of two promising ranging techniques: one based on received RF signal strength and the other based on the Time of Arrival (ToA) of RF and ultrasonic signals. Our experiments of distance discovery with RF signal strength were conducted on the WINS wireless sensor nodes [12] (figure 1) developed by the Rockwell Science Center (RSC). To perform our evaluation of ToA, we have designed and implemented a testbed of ultrasound-equipped sensor nodes,

called *Medusa* (from Greek mythology - a monster with many heads) nodes (figure 2). To address the variation of propagation characteristics of ultrasound from place to place AHLoS estimates the propagation characteristics on the fly in the actual deployment environment. The second part of our work uses the ranging techniques described above, to develop a set of distributed localization algorithms. Node positions are estimated using least squares estimation in an iterative multilateration process. This ability of AHLoS to estimate node locations in an ad-hoc setting with a few centimeters accuracy is demonstrated on a testbed comprised of first generation *Medusa* nodes. Error propagation, system scalability and energy consumption are studied through simulation.

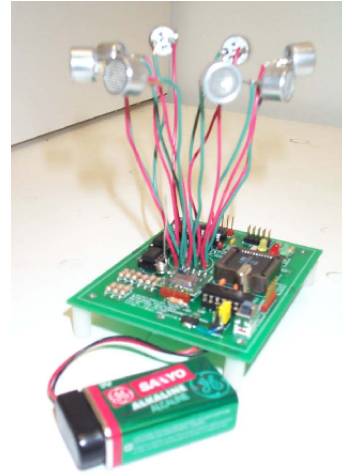


Figure 2: *Medusa* experimental node

1.3 Paper Organization

This paper is organized as follows: In the next section we provide some background on localization and we survey the related work. Section 3 presents the evaluation of our two candidate ranging methods: Received signal strength and time of arrival. Section 4 describes the localization algorithms and section 5 is a short study on node and beacon node placement. In section 6 we discuss our implementation and experiments. Section 7 discusses the tradeoffs between centralized and distributed localization and section 8 concludes this paper.

2. BACKGROUND AND RELATED WORK

2.1 Background

The majority of existing location discovery approaches consist of two basic phases: (1) distance (or angle) estimation and (2) distance (or angle) combining. The most popular methods for estimating the distance between two nodes are:

- **Received Signal Strength Indicator (RSSI)** techniques measure the power of the signal at the receiver. Based on the known transmit power, the effective propagation loss can be calculated. Theoretical and empirical models are used to translate this loss into a distance estimate. This method has been used mainly for RF signals.

- **Time based methods (ToA, TDoA)** record the time-of-arrival (ToA) or time-difference-of-arrival (TDoA). The propagation time can be directly translated into distance, based on the known signal propagation speed. These methods can be applied to many different signals, such as RF, acoustic, infrared and ultrasound.
- **Angle -of -Arrival (AoA)** systems estimate the angle at which signals are received and use simple geometric relationships to calculate node positions.

A detailed discussion of these methods can be found in [20]. For the combining phase, the most popular alternatives are:

- The most basic and intuitive method is called hyperbolic tri-lateration. It locates a node by calculating the intersection of 3 circles (figure 3a).
- Triangulation is used when the direction of the node instead of the distance is estimated, as in AoA systems. The node positions are calculated in this case by using the trigonometry laws of sines and cosines (figure 3b).
- The third method is Maximum Likelihood (ML) estimation (figure 3c). It estimates the position of a node by minimizing the differences between the measured distances and estimated distances. We have chosen this technique as the basis of AHLoS for obtaining the Minimum Mean Square Estimate(MMSE) from a set of noisy distance measurements.

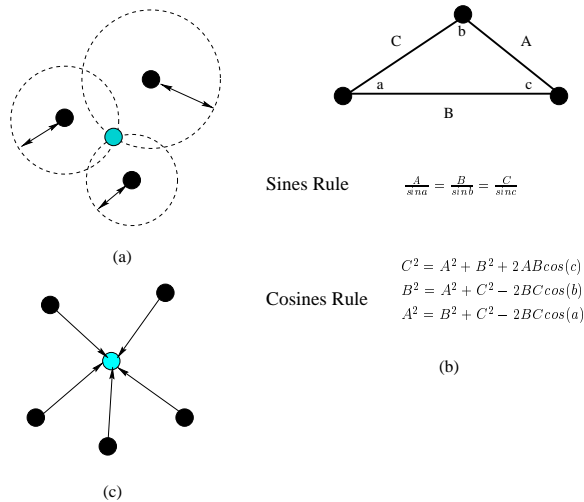


Figure 3: Localization Basics a) Hyperbolic tri-lateration, b) Triangulation, c) ML Multilateration

2.2 Related Work

In the past few decades, numerous localization systems have been developed and deployed. In the 1970s, the automatic vehicle location (AVL) systems were deployed to determine the position of police cars and military ground transportation vehicles. A set of stationary base stations acting as observation points use ToA and TDoA techniques to generate distance estimates. The vehicle position is then derived through multilaterations, using Taylor Series Expansion to transform a non-linear least squares problem to a

linear [7][8]. Similar approaches can also be found in military applications for determining the position of airplanes.

In 1993, the well-known Global Positioning System (GPS) [34] system was deployed, which is based on the NAVSTAR satellite constellation (24 satellites). LORAN [28] operates in a similar way to GPS but uses ground based beacons instead of satellites. In 1996, the U.S Federal Communications Commission (FCC) required that all wireless service providers give location information to the Emergency 911 services. Cellular base stations are used to locate mobile telephone users within a cell [9][10]. Distance estimates are generated with TDoA. The base station transmits a beacon and the handset reflects the signal back to the base station. Location information is again calculated by multilateration using least squares methods. By October 2001, FCC requires a 125-meter root mean square(RMS) accuracy in 67% of the time and by October 2006 a 300-meter RMS accuracy for 95% of the times is required.

Recently, there has been an increasing interest for indoor localization systems. The RADAR system [1] can track the location of users within a building. To calculate user locations the RADAR system uses RF signal strength measurements from three fixed base stations in two phases. First, a comprehensive set of received signal strength measurements is obtained in an offline phase to build a set of signal strength maps. The second phase is an online phase during which the location of users can be obtained by observing the received signal strength from the user stations and matching that with the readings from the offline phase. This process, eliminates multipath and shadowing effects at the cost of considerable preplanning effort.

The Cricket location support system [4] is also designed for indoor localization. It provides support for context aware applications and is low cost. Unlike the systems discussed so far, it uses ultrasound instead of RF signals. Fixed beacons inside the building distribute geographic information to the listener nodes. Cricket can achieve a granularity of 4 by 4 feet. Room level granularity can be obtained by the active badge [22] system, which uses infrared signals. The next development in this area on indoor localization is BAT [29] [30]. A BAT node carries an ultrasound transmitter whose signals are picked up by an array of receivers mounted on the ceiling. The location of a BAT can be calculated via multilateration with a few centimeters of accuracy. An RF base station coordinates the ultrasound transmissions such that interference from nearby transmitters is avoided. This system relies heavily on a centralized infrastructure.

In the ad-hoc domain, fewer localization systems exist. An RF based proximity method is presented in [21], in which the location of a node is given as a centroid. This centroid is generated by counting the beacon signals transmitted by a set of beacons pre-positioned in a mesh pattern. A different approach is taken in the Picoradio project at UC Berkeley. It provides a geolocation scheme for an indoor environment [11], based on RF received signal strength measurements and pre-calculated signal strength maps.

Our system, AHLoS, also belongs to the ad-hoc class. Although uses RF and ultrasound transmissions similar to the

Cricket and BAT Systems, it also has some key differences. AHLoS does not rely on a preinstalled infrastructure. Instead, it is a fully ad-hoc system with distributed localization algorithms running at every node. This results in a flexible system that only requires a small initial fraction of the nodes to be aware of their locations. Furthermore, it enables nodes to estimate their locations even if they are not within range with the beacon nodes. From a power awareness perspective, it also ensures that all nodes play an equal role in the location discovery process resulting in an even distribution of power consumption. The resulting localization system provides fine-grained localization with an accuracy of a few centimeters, similar to the BAT system without requiring infrastructure support. Finally, unlike all the systems discussed so far, AHLoS provisions for dynamic on-line estimation of the ultrasound propagation characteristics. This renders our approach extremely robust even in the presence of changing environments.

3. RESEARCH METHODOLOGY

As a first step in our study, we characterize the *ranging* capabilities of our two target technologies: Received RF signal strength using the WINS nodes and RF and ultrasound ToA using the *Medusa* nodes.

3.1 Ranging Characterization

3.1.1 Received Signal Strength

The signal strength method uses the relationship of RF signal attenuation as a function of distance. From this relationship a mathematical propagation model can be derived. From detailed studies of the RF signal propagation characteristics [18], it is well known that the propagation characteristics of radio signals can vary with changes in the surrounding environment (weather changes, urban / rural and indoor / outdoor settings). To evaluate signal strength measurements we conducted some experiments with the target system of interest, the WINS sensor nodes [12]. The WINS nodes have a 200MHz StrongARM 1100 processor, 1MB Flash, 128KB RAM and the Hummingbird digital cordless telephony (DECT) radio chipset that can transmit at 15 distinct power levels ranging from -9.3 to 15.6 dBm (0.12 to 36.31 mW). The WINS nodes carry an omni-directional antenna hence the radio signal is uniformly transmitted with the same power in all directions around the node. As part of the radio architecture, the WINS nodes provide a pair of RSSI (Received Signal Strength Indicators) resistors. RSSI registers are a standard feature in many wireless network cards [23]. Using these registers we conducted a set of measurements in order to derive an appropriate model for ranging. We performed measurements in several different settings (inside our lab, in the parking lot and between buildings). Unfortunately, a consistent model of the signal attenuation as a function of distance could not be obtained. This is mainly attributed to multipath, fading and shadowing effects. Another source of inconsistency is the great variation of RSSI associated with the altitude of the radio antenna. For instance, at ground level, the radio range at the maximum transmit power level the usable radio transmission range is around 30m whereas when the node is placed at a height of 1.5m the usable transmission range increases to around 100m. Because of these inconsistencies, we were only able to derive a model for an idealized setting; in a football

field with all the nodes positioned at ground level. For this setup we developed a model based on the RSSI register readings at different transmission power levels and different node separations.

A model (equation 1) is derived by obtaining a least square fit for each power level. P_{RSSI} is the RSSI register reading and r is the distance between two nodes. Parameters X and n are constants that can be derived as functions of distance r for each power level. Averaged measurements and the corresponding derived models are shown in figure 4. Table 1 gives the X and n parameters for each case.

$$P_{RSSI} = \frac{X}{r^n} \quad (1)$$

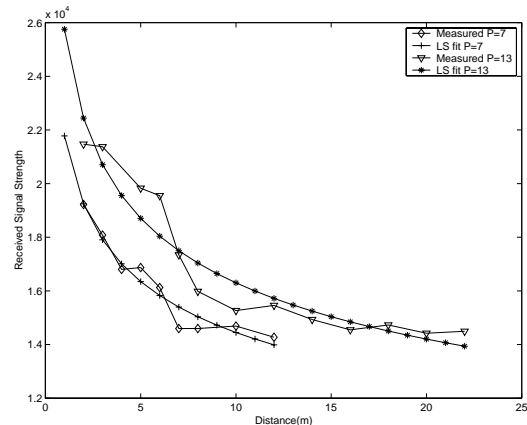


Figure 4: Radio Signal Strength Radio Characterization using WINS nodes (power levels P=7,13)

Table 1: RSSI Ranging Model Parameters for WINS nodes

Power Level	dBm	mW	X	n
7	2.5	1.78	21778.338	0.178186
13	14.4	27.54	25753.63	0.198641

With all the nodes placed on a flat plane, signal strength ranging can provide a distance estimate with an accuracy of a few meters. In all other cases, this experiment has shown that the use of radio signal strength can be very unpredictable. Another problem with the received signal strength approach is that radios in sensor nodes are low cost ones without precise well-calibrated components, such as the DECT radios in Rockwell's nodes or the emerging Bluetooth radios. As a result, it is not unusual for different nodes to exhibit significant variation in actual transmit power for the same transmit power level, or in the RSSI measured for the same actual received signal strength. Differences of several dBs are often seen. While these variations are acceptable for using transmit power adaptation and RSSI measurements for link layer protocols, they do not provide the accuracy required for fine-grained localization. A potential solution

would be to calibrate each node against a reference node prior to deployment, and store gain factors in non-volatile storage so that the run-time RSSI measurements may be normalized to a common scale.

3.1.2 ToA using RF and Ultrasound

To characterize ToA ranging on the *Medusa* nodes we measure the time difference between two simultaneously transmitted radio and ultrasound signals at the receiver (figure 5).

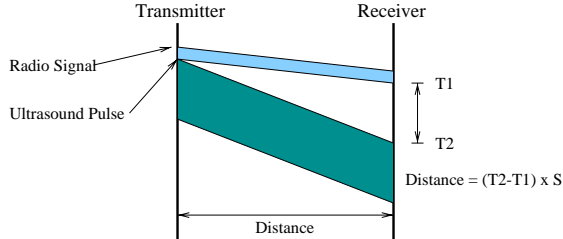


Figure 5: Distance measurement using ultrasound and radio signals

The ultrasound range on the *Medusa* nodes is about 3 meters (approximately 11-12 feet). We found this to be a convenient range for performing multihop experiments in our lab but we note that longer ranges are also possible at higher cost and power premiums. The Polaroid 6500 ultrasonic ranging module [17] for example has a range of more than 10 meters (the second generation of *Medusa* nodes will have a 10-15 meter range). We characterize ToA ranging by using two *Medusa* nodes placed on the floor of our lab. We recorded the time difference of arrival at 25-centimeter intervals. The results of our measurements are shown in figure 6. The x axis represents distance in centimeters and the y axis represent the microcontroller timer counter value.

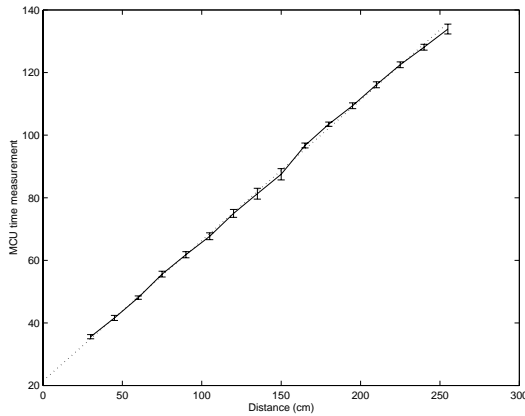


Figure 6: Ultrasound Ranging Characterization

The speed of sound is characterized in terms of the microcontroller timer ticks. To estimate the speed to sound as a function of microcontroller time, we perform a best line fit using linear regression (equation 2). s is the speed of sound in timer ticks, d is the estimated distance between 2

nodes and k is a constant. For this model $s = 0.4485$ and $k = 21.485831$.

$$t = sd + k \quad (2)$$

This *ranging* system can provide an accuracy of 2 centimeters for node separations under 3 meters. Like the RF signals, ultrasound also suffers from multipath effects. Fortunately, they are easier to detect. ToA measurement use the first pulse received ensuring that the shortest path (straight line) reading is observed. Reflected pulses from nodes that do not have direct line of sight are filtered out using statistical techniques similar to the ones used in [30].

3.2 Signal Strength vs. ToA ranging

On comparing the two ranging alternatives, we found that ToA using RF and ultrasound is more reliable than received signal strength. While received signal strength is greatly affected by amplitude variations of the received signal, ToA ranging only depends on the time difference, a much more robust metric. Based on our characterization results we chose ToA as the primary ranging method for AHLoS. Similar to RF signals, the ultrasound signal propagation characteristics may change with variations in the surrounding environment. To minimize these effects, AHLoS dynamically estimates the signal propagation characteristics every time sufficient information is available. This ensures that AHLoS will operate in many diverse environments without prior calibration. If the sensor network is deployed over a large field, the signal propagation characteristics may vary from region to region across the field. The calculation of the ultrasound propagation characteristics in the locality of each node ensures better location estimates accuracy. Table 2 summarizes the comparison between signal strength and ultrasound ranging. One possible solution we are considering for our future work is to combine received signal strength and ToA methods. Since the received signal strength method has the same effective range as the radio communication range, it can be used to provide a proximity indication in places where the network connectivity is very sparse for ToA localization to take place. The ultrasound approach will provide fine grained localization in denser parts of the networks. For this configuration, we plan to have the *Medusa* boards act as *location coprocessors* for the WINS nodes.

4. LOCALIZATION ALGORITHMS

Given a *ranging* technology that estimates node separation we now describe our localization algorithms. These algorithms operate on an ad-hoc network of sensor nodes where a small percentage of the nodes are aware of their positions either through manual configuration or using GPS. We refer to the nodes with known positions as *beacon* nodes and those with unknown positions as *unknown* nodes. Our goal is to estimate the positions of as many *unknown* nodes as possible in a fully distributed fashion. The proposed location discovery algorithms follow an iterative process. After the sensor network is deployed, the *beacon* nodes broadcast their locations to their neighbors. Neighboring *unknown* nodes measure their separation from their neighbors and use the broadcasted *beacon* positions to estimate their own positions. Once an *unknown* node estimates its position, it becomes a *beacon* and broadcasts its estimated position to other nearby *unknown* nodes, enabling them to estimate their positions. This process repeats until all the *unknown*

Table 2: A comparison of RSSI and ultrasound ranging

Property	RSSI	Ultrasound
Range	same as radio communication range	3 meters (up to a few 10s of meters)
Accuracy	O(m), 2-4m for WINS	O(cm), 2cm for Medusa
Measurement Reliability	hard to predict, multipath and shadowing	multipath mostly predictable,time is a more robust metric
Hardware Requirements	RF signal strength must be available to CPU	ultrasound transducers and amplifier circuitry
Additional Power Requirements	none	tx and rx signal amplification
Challenges	large variances in RSSI readings, multipath, shadowing, fading effects	interference, obstacles, multipath

nodes that satisfy the requirements for multilateration obtain an estimate of their position. This process is defined as *iterative multilateration* which uses *atomic multilateration* as its main primitive. In the following subsections we provide the details of atomic and iterative multilateration. Furthermore, we describe *collaborative multilateration* as an additional enhanced primitive for iterative multilateration and we provide some suggestions for further optimizations.

4.1 Atomic Multilateration

Atomic multilateration makes up the basic case where an *unknown* node can estimate its location if it is within range of at least three beacons. If three or more beacons are available, the node also estimates the ultrasound speed of propagation for its locality. Figure 7a illustrates a topology for which atomic multilateration can be applied.

The error of the measured distance between an unknown node and its *i*th beacon can be expressed as the difference between the measured distance and the estimated Euclidean distance (equation 3). x_0 and y_0 are the estimated coordinates for the unknown node 0 for $i = 1, 2, 3 \dots N$, where N is the total number of beacons, and t_{i0} is the time it takes for an ultrasound signal to propagate from beacon i to node 0, and s is the estimated ultrasound propagation speed.

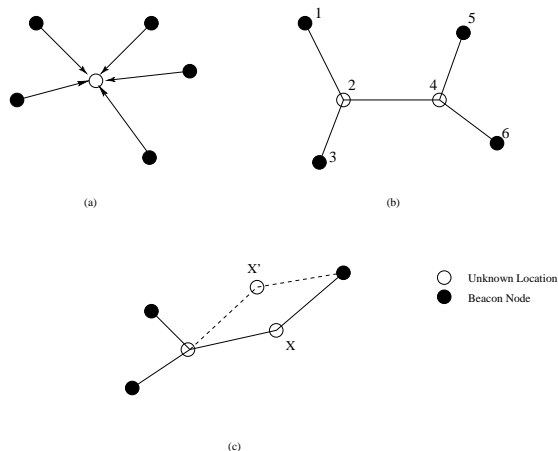


Figure 7: Multilateration examples

$$f_i(x_0, y_0, s) = st_{i0} - \sqrt{(x_i - x_0)^2 + (y_i - y_0)^2} \quad (3)$$

Given that an adequate number of beacon nodes are available, a Maximum Likelihood estimate of the node's position can be obtained by taking the minimum mean square estimate (MMSE) of a system of $f_i(x_0, y_0, s)$ equations (equation 4). Term α represents the weight applied to each equation. For simplicity we assume that $\alpha = 1$.

$$F(x_0, y_0, s) = \sum_{i=1}^N \alpha^2 f(i)^2 \quad (4)$$

If a node has three or more beacons a set of three equations of the form of (3) can be constructed yield an over-determined system with a unique solution for the position of the unknown node 0. If four or more beacons are available, the ultrasound propagation speed s can also be estimated. The resulting system of equations can be linearized by setting $f_i(x_0, y_0, s) =$ equation 3, squaring and rearranging terms to obtain equation 5.

$$-x_i^2 - y_i^2 = (x_0^2 + y_0^2) + x_0(-2x_i) + y_0(-2y_i) - s^2 t_{i0}^2 \quad (5)$$

for k such equations we can eliminate the $(x_0^2 + y_0^2)$ terms by subtracting the k th equation from the rest.

$$-x_i^2 - y_i^2 + x_k^2 + y_k^2 = 2x_0(x_k - x_i) + 2y_0(y_k - y_i) + s^2(t_{ik}^2 - t_{i0}^2) \quad (6)$$

this system of equations has the form $y = bX$ and can be solved using the matrix solution for MMSE [25] given by $b = (X^T X)^{-1} X^T y$ where

$$X = \begin{bmatrix} 2(x_k - x_1) & 2(y_k - y_1) & t_{k0}^2 - t_{k1}^2 \\ 2(x_k - x_2) & 2(y_k - y_2) & t_{k0}^2 - t_{k2}^2 \\ \vdots & \vdots & \vdots \\ 2(x_k - x_{k-1}) & 2(y_k - y_{k-1}) & t_{k0}^2 - t_{k(k-1)}^2 \end{bmatrix}$$

$$y = \begin{bmatrix} -x_1^2 - y_1^2 + x_k^2 + y_k^2 \\ -x_2^2 - y_2^2 + x_k^2 + y_k^2 \\ \vdots \\ x_{k-1}^2 - y_{k-1}^2 + x_k^2 + y_k^2 \end{bmatrix}$$

and

$$b = \begin{bmatrix} x_0 \\ y_0 \\ s^2 \end{bmatrix}$$

Based on this solution we define the following requirement for atomic multilateration.

REQUIREMENT 1. *Atomic multilateration can take place if the unknown node is within one hop distance from at least three beacon nodes. The node may also estimate the ultrasound propagation speed if four or more beacons are available.*

Although requirement 1 is necessary for atomic multilateration, it is not always sufficient. In the special case when beacons are in a straight line, a position estimate cannot be obtained by atomic multilateration. If this occurs, the node will attempt to estimate its position using collaborative multilateration. We also note that atomic multilateration can be performed in 3-D without requiring an additional beacon [33].

4.2 Iterative Multilateration

The *iterative multilateration* algorithm uses atomic multilateration as its main primitive to estimate node locations in an ad-hoc network. This algorithm is fully distributed and can run on each individual node in the network. Alternatively, the algorithm can also run at a single central node or a set of cluster-heads, if the network is cluster based. Figure 8 illustrates how iterative multilateration would execute from a central node that has global knowledge of the network. The algorithm operates on a graph G which represents the network connectivity. The weights of the graph edges denote the separation between two adjacent nodes. The algorithm starts by estimating the position of the unknown node with the maximum number of beacons using atomic multilateration. Since at a central location all the the entire network topology is known so we start from the *unknown* node with the maximum number of beacons to obtain better accuracy and faster convergence (in the distributed version an *unknown* will perform a multilateration as soon as information from three beacons). When an *unknown* node estimates its location, it becomes a *beacon*. This process repeats until the positions of all the nodes that eventually can have three or more beacons are estimated.

```

boolean iterativeMultilateration (G)
(MaxBeaconNode, BeaconCount) ← unknown
node with most beacons
while BeaconCount ≥ 3
set Beacon (MaxBeaconNode)
(MaxBeaconNode, BeaconCount) ← unknown
node with most beacons

```

Figure 8: Iterative Multilateration Algorithm as it executes on a centralized node

A drawback of iterative multilateration is the error accumulation that results from the use of *unknown* nodes that estimate their positions as *beacons*. Fortunately, this error accumulation is not very high because of the high precision of our ranging method. Figure 9 shows the position errors in a simulated network of 50 *Medusa* nodes when 10% of the nodes are initially configured as beacons. The nodes are deployed on a square grid of side 15 meters. The simulation considers two types of errors: 1) ranging errors and 2) beacon placement errors. In both cases a 20mm white Gaussian error is used. In both cases the estimated node positions are within 20 cm from the actual positions.

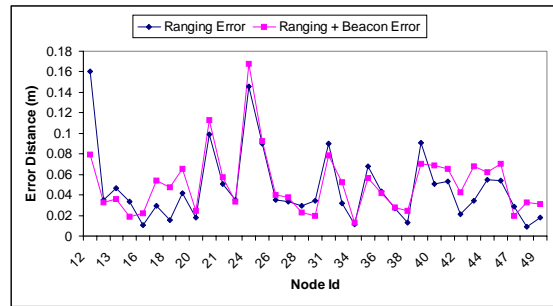


Figure 9: Iterative Multilateration Accuracy in a network of 50 nodes and 10% beacons

4.3 Collaborative Multilateration

In an ad-hoc deployment with random distribution of *beacons*, it is highly possible that at some nodes, the conditions for atomic multilateration will not be met; i.e. an *unknown* node may never have three neighboring beacon nodes therefore it will not be able to estimate its position using *atomic multilateration*. When this occurs, a node may attempt to estimate its position by considering use of location information over multiple hops in a process we refer to as *collaborative multilateration*. If sufficient information is available to form an over-determined system of equations with a unique solution set, a node can estimate its position and the position of one or more additional unknown nodes by solving a set of simultaneous quadratic equations. Figure 7b illustrates one of the most basic topologies for which *collaborative multilateration* can be applied. Nodes 2 and 4 are *unknown* nodes, while nodes 1,3,5,6 are *beacon* nodes. Since both nodes 2 and 4 have three neighbors (degree $d = 3$) and all the other nodes are *beacons*, a unique position estimate for nodes 2 and 4 can be computed. More formally, collaborative multilateration can be stated as follows: Con-

sider the ad-hoc network to be a connected undirected graph $G = (N, E)$ consisting of $|N| = n$ nodes and a set E of $n - 1$ or more edges. The *beacon* nodes are denoted by a set B where $B \subseteq N$ and the set of *unknown* nodes is denoted by U where $U \subseteq G$. Our goal is to solve for

$x_u, y_u \forall u \subseteq U$ by minimizing

$$f(x_u, y_u) = D_{iu} - \sqrt{(x_i - x_u)^2 + (y_i - y_u)^2} \quad (7)$$

for all participating node pairs i, u where $i \subseteq B$ or $i \subseteq U$ and $u \subseteq U$. Subject to:

x_i, y_i are known if $i \subseteq B$, and every node pair i, u is a participating pair. Participating nodes and participating pair are defined as follows:

DEFINITION 1. *A node is a participating node if it is either a beacon or if it is an unknown with at least three participating neighbors.*

In figure 7b if collaborative multilateration starts at node 2, node 2 must have at least three participating neighbors. Nodes 1 and 3 are beacons therefore they are participating. Node 4 is unknown but has two beacons: nodes 5 and 6. Node 4 is also connected to node 2 thus making both of them participating nodes.

DEFINITION 2. *A participating node pair is a beacon-unknown or unknown-unknown pair of connected nodes where all unknowns are participating.*

In this formulation, the nodes participating in collaborative multilateration make up a subgraph of G , for which an equation of the form of 7 can be written for each edge E that connects a pair of participating nodes. To ensure a unique solution, all nodes considered must be participating. In figure 7b for example, we have five edges thus a set of five equations can be obtained. In some cases other cases, we may have a well-determined system of n equations and n unknowns such as in the case shown figure 7c. We can easily observe however, that node X can have two possible positions that would satisfy this system therefore the solution is not unique and node X is not a participating node. If the above conditions are met, the resulting system of non-linear equations can be solved with optimization methods such as gradient descend [26] and simulated annealing [27].

The algorithm in figure 10 provides a basic example of how a node determines whether it can initiate collaborative multilateration. The parameter *node* denotes the node id from where the search for a collaborative multilateration begins. The second parameter *callerId* holds the node id of the node that calls the particular instance of the function. *isInitiator* is a boolean variable that is set to *true* if the node was the initiator of the collaborative multilateration process and *false* otherwise. This is used to set the *limit* flag that drives the recursion.

```

boolean isCollaborative (node, callerId, isInitiator)
  if isInitiator==true limit ← 3
  else limit ← 2
  count ← beaconCount(node)
  if count ≥ limit return true
  for each unknown neighbor i not previously visited
    if isCollaborative (i, node, false) count++
  if count == limit return true
  return false

```

Figure 10: Algorithm for checking the feasibility for collaborative multilateration

Collaborative multilateration can be used to assist iterative multilateration in places of the network where the beacon density is low and the requirement for atomic multilateration is not satisfied. Figure 11 illustrates how iterative multilateration would call collaborative multilateration when the requirement for atomic multilateration is not met.

```

boolean iterativeMultilateration (G)
  (MaxBeaconNode, BeaconCount) ← unknown
  node with most beacons
  while BeaconCount ≥ 3
    setBeacon (MaxBeaconNode)
    (MaxBeaconNode, BeaconCount) ← unknown
    node with most beacons
    while isCollaborative (MaxBeaconNode, -1, true)
      set all nodes in collaborative set as beacons
      (MaxBeaconNode, BeaconCount) ← unknown
      node with most beacons
    while BeaconCount ≥ 3
      setBeacon (MaxBeaconNode)
      (MaxBeaconNode, BeaconCount) ← unknown
      node with most beacons

```

Figure 11: Enhanced Iterative Multilateration

Collaborative multilateration can help in situations where the percentage of beacons is low. This effect is shown in figure 12. This scenario considers a sensor field of 100 by 100 and a sensing range of 10 and two network sizes of 200 and 300 nodes. As shown in the figure, if the percentage of *beacons* is small, the number of node locations that can be resolved is substantially increased with collaborative multilateration. This result also shows how network density is related to the localization process. In the 300 node network, more node locations can be estimated than in the 200 node network with the same percentage of beacons. This is due to the higher degree of connectivity. The effects of node and beacon placement on the localization process is studied in more detail in section 5.

4.4 Further Optimizations

The accuracy of the estimated locations in the multilateration algorithms described in this section may be further improved with two additional optimizations. First, error

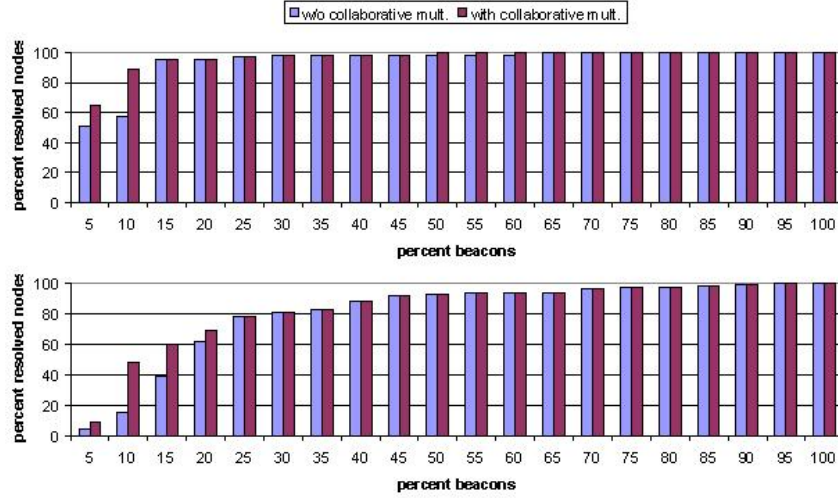


Figure 12: Effect of collaborative multilateration top, 300 nodes, bottom 200 nodes

propagation can be reduced by using weighted multilateration. In this scheme, beacons with higher certainty about their location are weighted more than beacons with lower certainty during a multilateration. As new nodes become beacons, the certainty of their estimated location can also be computed and used as a weight in future multilaterations. Additionally, by applying collaborative multilateration over a wider scope, the accumulated error can be reduced. The solution methodology and further evaluation of these optimizations are part of our future work and will be the subject of a future paper.

5. NODE AND BEACON PLACEMENT

The success of the location discovery algorithm depends on network connectivity and beacon placement. In this section, we conduct a brief probabilistic analysis to determine how the connectivity requirements can be met when nodes are uniformly deployed in a field. Based on these results, we later perform a statistical analysis to get an indication on the percentage of beacons required. When considering node deployment, the main metric of interest is the probability with which any node in the network has a degree of three or more, assuming that sensor nodes are uniformly distributed over the sensor field. In a network of N nodes deployed in a square field of side L , the probability $P(d)$ of a node having degree d is given by the binomial distribution in equation 8 and the probability P_R being in transmission range.

$$P(d) = P_R^d (1 - P_R)^{N-d-1} \binom{N-1}{d} \quad (8)$$

$$P_R = \frac{\pi R^2}{L^2} \quad (9)$$

For large values of N tending to infinity, the above binomial distribution converges to a Poisson distribution. When taking into account that $\lambda = N \cdot P_R$ we get equation 10, the

probability of a node have degree of three or more can be calculated. Also, an indication of the number of nodes required per unit area can be calculated in terms of λ . Table 3 shows the number of nodes required to cover a square field of size $L = 100$ and range $R = 10$ as well as the probability for a node to have degree greater than three or four for different values of λ . These probabilities are obtained from equation 11.

$$P(d) = \frac{\lambda^d}{d!} \cdot e^{-\lambda} \quad (10)$$

$$P(d \geq n) = 1 - \sum_{i=0}^{n-1} P(i) \quad (11)$$

Table 3: Probability of node degree for different λ values

λ	$P(d \geq 3)$	$P(d \geq 4)$	nodes/ $10,000m^2$
2	0.323324	0.142877	39
4	0.761897	0.56653	78
6	0.938031	0.848796	117
8	0.986246	0.95762	157
10	0.997231	0.989664	196
12	0.999478	0.997708	235
14	0.999906	0.999526	274
16	0.999984	0.999907	314
18	0.999997	0.999982	353
20	1	0.999997	392

The connectivity results in figure 13 show the probabilities of a node having 0,1,2 or 3 and more neighbors. In addition to node connectivity, we determine percentage of initial beacon nodes required for the convergence of the localization

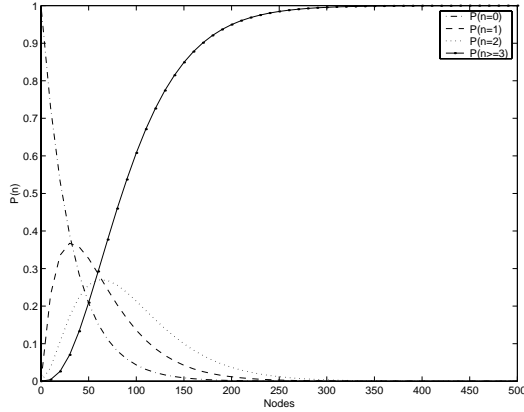


Figure 13: Connectivity result for a 100 x 100 field and sensor range 10

algorithm by statistical analysis. Using the same network setup as before, we report the percentage of nodes that estimate their locations while varying the percentage of nodes and beacons. The results in figure 14 are the averages over 100 simulations. The figure shows the percentage of beacons required to complete the iterative multilateration process using only atomic multilaterations. We note that the percentage of required beacons decreases as network density increases. Also as the network density increases, the transitions in the required number of beacons become much sharper since the addition of a few more beacon nodes reinforces the progress of the iterative multilateration algorithm.

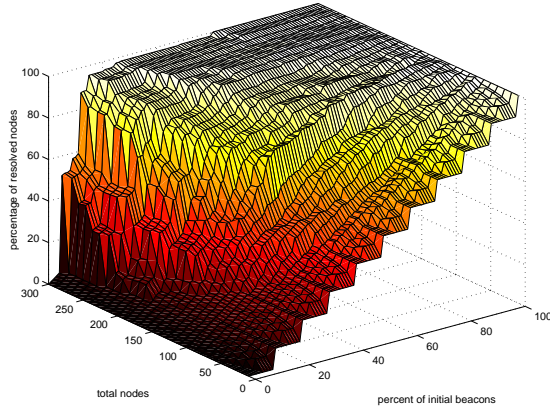


Figure 14: Beacon Requirements for different node densities

6. IMPLEMENTATION AND EXPERIMENTATION

6.1 Medusa Node Architecture

The *Medusa* node design (figure 2) is based on the AVR 8535 processor [13] which carries 8KB of flash memory, 512 bytes SRAM and 512 bytes of EEPROM memory. The radio we use is the DR3000 radio module from RF Monolithics[14]. This radio supports two data rates (2.4 and 19.2 kbps) and two modulation schemes (ASK and OOK). The ultrasound

circuitry consists of six (60 degree detect angle) pairs of 40KHz ultrasonic transducers arranged in a hexagonal pattern at the center of the board (note that for experimental purposes the *Medusa* node in figure 2 has 8 transducers). Each ultrasound transceiver is supported by a pair of solid core wires at an approximate height of 15 cm above the printed circuit board. We found this very convenient setup for experimentation since it allows the transceivers to be rotated in different directions. The first generation board is 3" x 4" and it is powered by a 9V battery. The *Medusa* firmware is based on an event driven firmware implementation suggested in [15]. The radio communication protocols use a variable size framing scheme, 4-6 bit encoding [16] and 16 bit CRC. The code for *ranging* is integrated in the ad-hoc routing protocol described in the next subsection.

6.2 Location Information Dissemination and Routing

In our experimental setup all measurements from the nodes are forwarded to a PC basestation. To route messages to the base station, we implemented a lightweight version of the DSDV [19] routing algorithm, which we refer to as DSDVlite. Instead of maintaining a routing table with the next hop information to every node, DSDVlite only maintains a short routing table that holds next hop information for the shortest route to gateway. Furthermore, this algorithm drives the localization process by carrying the location information of beacons, and by ensuring that the received ultrasound beacon signals originate from the same source node as the radio signals. The ultrasound beacon signal transmission begins right after the transmission of the start symbol for each routing packet. After this, the transmission of data and ultrasound signals proceed simultaneously. By ensuring that the duration of the data transmission is longer than the ultrasound transmission, the receiver can differentiate between erroneous ultrasound transmissions from other nodes. If the data packet is not correctly received because of a collision with another transmission, it also implies a collision of ultrasound signals hence the ultrasound time measurement is discarded.

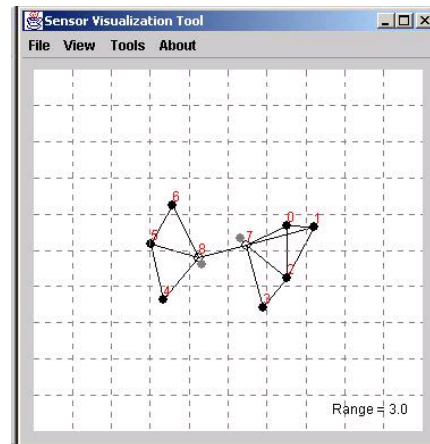


Figure 15: 9 node scenario

6.3 Experimental Setup

Our experimental testbed consists of 9 *Medusa* nodes and a Pentium II 300MHz PC. One node is configured as a gateway and it is attached to the PC through the serial port. Some of the nodes are pre-programmed with their locations and they act as beacons. All the nodes perform ranging and they transmit all the ranging information to the PC that runs the localization algorithms and displays the node positions on a sensor visualization tool. The node positions on the sensor visualization tool are updated at 5-second intervals. Figures 16 and 15 show some snapshots of node locations. The beacons are shown as black dots, the unknown nodes are white circles and the node position estimates are shown as gray dots. In all of our experiments all the node position estimates for each unknown node always fall within the 3" x 4" surface area of the *Medusa* boards.

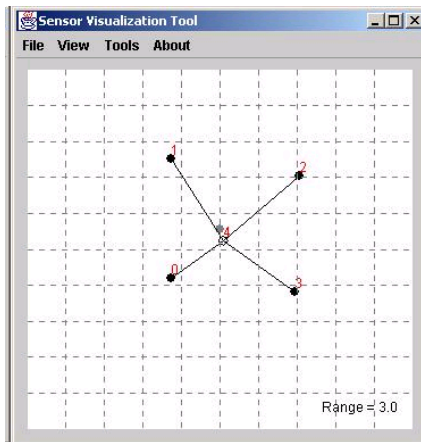


Figure 16: 5 node scenario

6.4 Power Characterization

In the previous subsection we verified the correct operation of our localization system. Our experimental setup will provide a reasonable solution for a small network but as the network scales, the traffic to the central gateway node will increase substantially. Before we can evaluate the tradeoffs between estimating locations at the nodes and estimating locations at a central node we first characterize power consumption of the *Medusa* nodes at different operational modes. Using an HP 1660 Logic Analyzer, a bench power supply and a high precision resistor we characterized the RFM radio and the AVR microcontroller on the *Medusa* nodes.

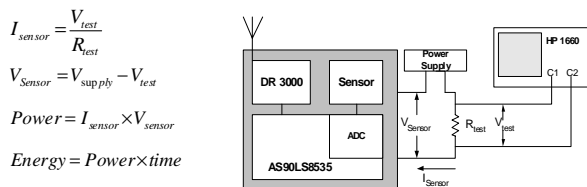


Figure 17: Power and Energy Relationships and Measurement Setup

The measurement setup and power/energy relationships are

shown in figure 17. The power consumption for different modes of the AVR microcontroller are shown in table 4. The power consumption for the different modes of the RFM radio are shown in figure 18 and table 5.

Table 4: AVR 8535 Power Characterization

AVR Mode	Current	Power
Active	2.9mA	8.7mW
Sleep	1.9mA	5.9mW
Power Down	1μA	3μW

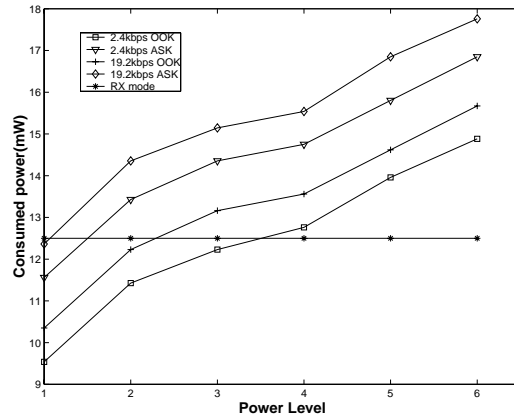


Figure 18: RFM Radio power consumption at different operational modes

7. TRADEOFFS BETWEEN CENTRALIZED AND DISTRIBUTED SCHEMES

One important aspect that needs to be determined is whether the location estimation should be done in a centralized or distributed fashion. In the former case, all the ranging measurements and beacon locations are collected to a central base station where the computation takes place and the results are forwarded back to the nodes. In the latter, each node estimates its own location when the requirements for atomic multilateration are met. For the AHLoS system, we advocate that distributed computation would be a better choice since a centralized approach has several drawbacks. First, to forward the location information to a central node, a route to the central node must be known. This implies the use of a routing protocol other than location based routing and also incurs some additional communication cost which is also affected by the efficiency of the existing routing and media access control protocols. Second, a centralized approach, creates a time synchronization problem. Whenever there is a change in the network topology the node's knowledge of location will not instantaneously updated. To correctly keep track of events, the central node will need to cache node locations to ensure consistency of event reports in space and time. Third, the placement of the central node implies some preplanning to ensure that the node is easily accessible by other nodes. Also, because of the large volume of traffic to and from the central node, the battery lifetime of the nodes around the central node will be seriously impacted. Fourth, the robustness of the system suffers. If the routes to the central node are broken, the nodes will

Table 5: RFM Power Characterization

Mode	Power Level	OOK Modulation				ASK Modulation			
		2.4Kbps		19.2Kbps		2.4Kbps		19.2Kbps	
		mA	mW	mA	mW	mA	mW	mA	mW
Tx	0.7368	4.95	14.88	5.22	15.67	5.63	16.85	5.95	17.76
Tx	0.5506	4.63	13.96	4.86	14.62	5.27	15.80	5.63	16.85
Tx	0.3972	4.22	12.76	4.49	13.56	4.90	14.75	5.18	15.54
Tx	0.3307	4.04	12.23	4.36	13.16	4.77	14.35	5.04	15.15
Tx	0.2396	3.77	11.43	4.04	12.23	4.45	13.43	4.77	14.35
Tx	0.0979	3.13	9.54	3.40	10.35	3.81	11.56	4.08	12.36
Rx	-	4.13	12.50	4.13	12.50	4.13	12.50	4.13	12.50
Idle	-	4.08	12.36	4.08	12.36	4.08	12.36	4.08	12.36
Sleep	-	0.005	0.016	0.005	0.016	0.005	0.016	0.005	0.016

not be able to communicate their location information to the central node and vice versa. Finally, since all the raw data is required, the data aggregation that can be performed within the network to conserve communication bandwidth is minimal. One advantage of performing the computation at a centralized location is that more rigorous localization algorithms can be applied such as the one presented in [35]. Such algorithms however require much more powerful computational capabilities than the ones available at low cost sensor nodes. Overall, a centralized implementation will not only reduce the network lifetime but it will also increase its complexity and compromise its robustness. On the other hand, if location estimation takes place at each node in a distributed manner the above problems can be alleviated. Topology changes will be handled locally and the location estimate at each node can be updated at minimal cost. In addition, the network can operate totally on location based routing so the implementation complexity will be reduced. Also since each node is responsible for determining its location, the localization is more tolerant to node failures.

To evaluate energy consumption tradeoffs between the centralized and distributed approaches we run some simulations on a typical sensor network setup. In our scenario the central node is placed at the center of a square sensor field. Furthermore, we assume the use of an ideal, medium access control(MAC) and routing protocols. The MAC protocol is collision free and the routing protocol always uses the shortest route to the central node. The total number of bytes transmitted by all the nodes during both distributed and centralized localization is recorded. The network size varied with the network density kept constant by using a value of $\lambda = 6$ or 117 nodes for every $10,000m^2$ (from table 3). The simulation setup considers the same packet sizes as the implementation on the medusa nodes. For the centralized system each node forwards the range measurements between all its neighbors. If the node is *beacon* it also forwards its location information (this is 96 bits long which is equivalent to a GPS reading). Once the location is computed, the central node will forward the results back to node the corresponding unknown nodes. In the distributed setup, each node transmits a short beacon signal (radio and ultrasound pulse) followed by the senders location if the sender is a beacon. In both cases, the simulation runs for one full cycle of the localization process(until all feasible unknown node

positions are resolved). The average number of transmitted bytes for each case are shown in figures 19 and 20 for 10% and 20% beacon density respectively. The results shown in the figure are averages of over 100 simulations with random node placement following a uniform distribution.

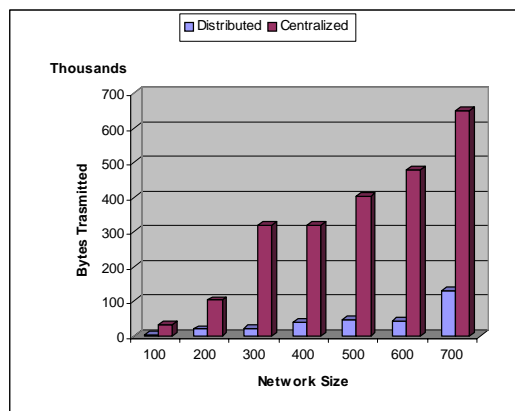
**Figure 19: Traffic in distributed and centralized implementations with 10% beacons**

Figure 21 shows the average energy consumption per node for the *Medusa* nodes when the radio transmission power is set to 0.24mW. This result is based on the power characterization of the *Medusa* nodes from the previous section. We also note that the energy overhead for the ultrasound based ranging is the same for both centralized and distributed schemes therefore it is not included in the energy results presented here. These results show that in the distributed setup has six to ten times less communication overhead than the centralized setup. Another interesting trend to note is that in the centralized setup, network traffic increases as the percentage of *beacon* nodes increases. In the distributed setup however, the traffic decreases as the percentage of *beacon* nodes increases. This decrease in traffic is mainly attributed to the fact that most of the times the localization process can converge faster if more beacon nodes are available; hence less information exchange has to take place between the nodes.

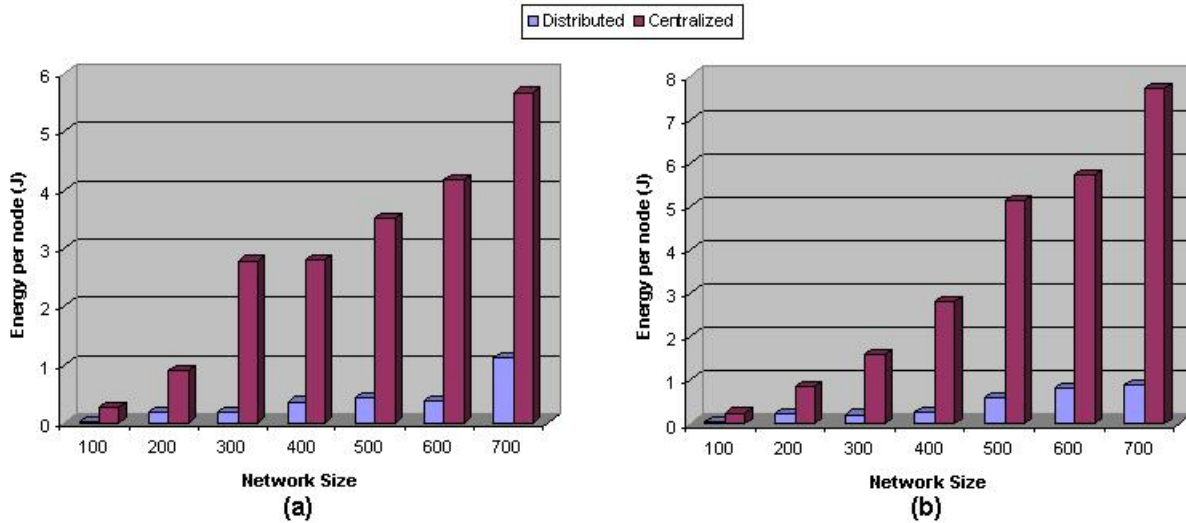


Figure 21: Average energy spent at a node during localization with a) 10% beacons, b) 20% beacons

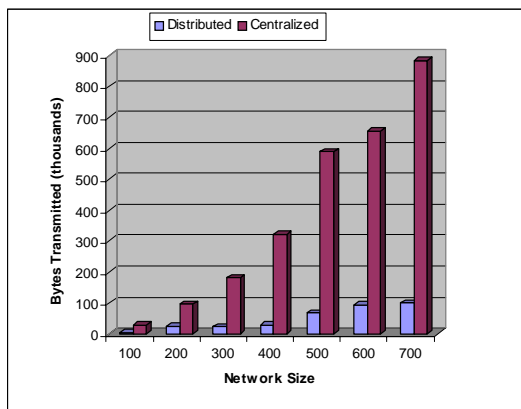


Figure 20: Traffic in distributed and centralized implementations with 20% beacons

8. CONCLUSIONS

We have presented a new localization scheme for wireless ad-hoc sensor networks. From our study we found that the use of ToA ranging is a good candidate for fine-grained localization as it is less sensitive to physical effects. Received RF signal strength ranging on the other hand is not suitable for fine-grained localization. Furthermore, we conclude that our fine-grained localization scheme should operate in a distributed fashion. Although more accurate location estimations can be obtained with centralized implementation, a distributed implementation will increase the system robustness and will result in a more even distribution of power consumption across the network during localization. Furthermore, the implementation of our testbed proved to be an indispensable tool for understanding and analyzing the strengths and limitations of our approach. Although our system performed very well for our experiments, we recommend the use of a more powerful CPU on the on the

sensor nodes for the following reasons. First, RF and ultrasound ToA ranging requires the use of a dedicated high speed timer. In our implementation the 4MHz AVR microcontroller is dedicated to localization and this is sufficient. If however, the microcontroller is expected to perform additional tasks at the same time a higher performance processor is highly recommended. Based on our experience, we are currently developing a second generation of the *Medusa* nodes. These nodes will be capable of performing hybrid ranging by introducing the fusion of both ultrasonic ToA ranging and received signal strength RF ranging. Finally, in this initial study we found that the accuracy of iterative multilateration is satisfactory for small networks but needs to be improved for larger scale networks. To this end, as part of our future work we plan to extend our algorithms to achieve better accuracy by limiting the error propagation across the network.

Acknowledgments

This paper is based in part on research funded through NSF under grant number ANI-008577, and through DARPA SensIT and Rome Laboratory, Air Force Material Command, USAF, under agreement number F30602-99-1-0529. The U.S. Government is authorized to reproduce and distribute reprints for Governmental purposes notwithstanding any copyright annotation thereon. Any opinions, findings, and conclusions or recommendations expressed in this paper are those of the authors and do not necessarily reflect the views of the NSF, DARPA, or Rome Laboratory, USAF. We also thank the anonymous reviews for their detailed feedback and suggestions.

9. REFERENCES

- [1] P. Bahl, V. Padmanabhan, *RADAR: An In-Building RF-based User Location and Tracking System* Proceedings of INFOCOM 2000 Tel Aviv, Israel, March 2000, p775-84, vol. 2
- [2] AVL Information Systems, Inc ,

<http://www.avlinfosys.com/>

- [3] Deborah Estrin, Ramesh Govindan and John Heidemann, *Scalable Coordination in Sensor Networks* Proceedings of Fifth Annual ACM/IEEE International Conference on Mobile Computing and Networking, Seattle, WA, Aug 1999, p263-70
- [4] N. Priyantha, A. Chakraborty and H. Balakrishnan, *The Cricket Location-Support System*, Proceedings of International Conference on Mobile Computing and Networking, pp. 32-43, August 6-11, 2000, Boston, MA
- [5] J. Li, J. Jannotti, D. S. J. DeCouto, D. R. Karger and R. Morris *A Scalable Location Service for Geographic Ad-Hoc Routing* Proceedings of ACM Mobile Communications Conference, August 6-11 2000, Boston, Massachusetts
- [6] K. Amouris, S. Papavassiliou, M. Li *A Position-Based Multi-Zone Routing Protocol for Wide Area Mobile Ad-Hoc Networks*, Proceedings of VTC 99
- [7] G. Turing, W. Jewell and T. Johnston, *Simulation of Urban Vehicle-Monitoring Systems* IEEE Transactions on Vehicular Technology, Vol VT-21, No1. Page 9-16, February 1972
- [8] W. Foy *Position-Location Solution by Taylor Series Estimation* IEEE Transactions of Aerospace and Electronic Systems Vol. AES-12, No. 2, pages 187-193, March 1976
- [9] J. Caffery and G. Stuber, *Subscriber Location in CDMA Cellular Networks* IEEE Transactions on Vehicular Technology, Vol. 47 No.2, pages 406-416, May 1998
- [10] J. Caffery and G. Stuber, *Overview of Radiolocation in CDMA Cellular Systems* IEEE Communications Magazine, April 1999
- [11] J. Beutel, *Geolocation in a PicoRadio Environment* Masters Thesis, UC Berkeley. July 1999.
- [12] Wireless Intergated Network Systems(WINS) <http://wins.rsc.rockwell.com/>
- [13] Atmel AS90LS8535, <http://www.atmel.com/atmel/products/prod200.htm>
- [14] DR3000 ASH Radio Module, <http://www.rfm.com/products/data/dr3000.pdf>
- [15] M. Melkonian, *Getting by without an RTOS* Embedded Systems Programming, September 2000
- [16] RFM Software Designer's Guide, <http://www.rfm.com/corp/apnotes.htm>
- [17] Polaroid 6500 ultrasonic ranging kit, <http://www.acroname.com/robotics/parts/R11-6500.html>
- [18] T. Rappaport *Wireless Communications Principle and Practice* Prentice Hall, 1996
- [19] C. Perkins and P. Bhagwat, *Highly Dynamic Destination Sequenced Distance-Vector Routing* In proceedings of the SIGCOMM 94 Conference on Communication Architectures, Protocols and Applications, pages 234-244, August 1994.
- [20] J. Gibson, *The Mobile Communications Handbook* IEEE Press 1999
- [21] N. Bulusu, J. Heidemann and D. Estrin, *GPS-less Low Cost Outdoor Localization For Very Small Devices*, IEEE Personal Communications Magazine, Special Issue on Networking the Physical World, August 2000.
- [22] R. Want, A. Hopper, V. Falcao and J. Gibbons, *The Active Badge Location System*. ACM Transactions on Information Systems 10, January 1992, pages 91-102
- [23] WaveLAN White specs, www.wavelan.com products
- [24] UCB/LBNL/VINT Network Simulator - ns (version 2) <http://www.isi.edu/nsnam/ns/>
- [25] W. Greene, *Econometric Analysis*, Third Edition, Prentice Hall 1997
- [26] D. J. Dayley and B. M. Bell, *A Method for GPS Positioning* IEE Trans., Aerosp. Electron. Syst., 1996, 32,(3),pp. 1148-54
- [27] W. H. Press, et al. *Numerical recipes in C: the art of scientific computing, 2nd ed.*. Cambridge ; New York: Cambridge University Press, 1992.
- [28] *LORAN* <http://www.navcen.uscg.mil/loran/Default.htm#Link>
- [29] A. Harter, A. Hopper, P. Steggle, A. Ward and P. Webster, *The Anatomy of a Context Aware Application* In Proceedings ACM/IEEE MOBICOM (Seattle, WA, Aug 1999)
- [30] A. Harter, A. Hooper *A New Location Technique for the Active Office* IEEE Personal Communications vol 4,(No. 5), October 1997, pp. 42-47
- [31] S. Meguerdichian , F. Koushanfar, M. Potkonjak and M. B. Srivastava *Coverage Problems in Wireless Ad-hoc Sensor Networks*, In proceedings of Infocom 2001, Ankorange, Alaska
- [32] M. B. Srivastava , R. Muntz and M. Potkonjak, *Smart Kindergarten: Sensor-based Wireless Networks for Smart Developmental Problem-solving Environments* In Proceedings of ACM/IEEE MOBICOM 2001
- [33] D. E. Manolakis, *Efficient Solution and Performance Analysis of 3-D Position Estimation by Trilateration* IEEE Transactions on Aerospace and Electronic Systems vol 32, p1239-48, October 1996
- [34] E. Kaplan, *Understanding GPS Principles and Applications* Artech House, 1996
- [35] L. Doherty, K. Pister and L. E. Ghaoui, *Convex Optimization Methods for Sensor Node Position Estimation* Proceedings of INFOCOM 2001, Anchorage, Alaska, April 2001